*Nuclear Quadrupole Resonance Study of a One-dimensional XY System: a Review (1,2) of Chlorine NQR in $PrCl_3$**

Robin L. Armstrong

Department of Physics
University of Toronto
Toronto M5S 1A7 Canada

D. R. Taylor

Department of Physics
Queen's University
Kingston K7L 3N6 Canada

I. INTRODUCTION

Crystals containing unpaired electron spins whose coupling is predominantly between nearest neighbors along chains provide physical systems for testing theoretical predictions for both the static and dynamic properties of idealized one-dimensional (1-D) chains. The Hamiltonian for a chain of spin 1/2 particles aligned along the z-axis is

$$H = J_{\parallel} \sum_i S_z^i S_z^{i+1} + J_{\perp} \sum_i (S_x^i S_x^{i+1} + S_y^i S_y^{i+1})$$

where $J_{\parallel}$ and $J_{\perp}$ are coupling constants parallel and perpendicular to the direction of the chain. The limiting case

$$H = J \sum_i (S_x^i S_x^{i+1} + S_y^i S_y^{i+1})$$

corresponds to what is called the XY chain. The hexagonal compound $PrCl_3$ provides a good approximation to the 1-D XY chain.

The structure of $PrCl_3$ is illustrated in Figure 1. Nearest neighbor Pr ions form chains along the hexagonal axis. Each Pr ion has nine close Cl neighbors which form three equilateral triangles; one triangle lies in the plane perpendicular to the hexagonal axis passing through the Pr ion, and the other two triangles are located above and below the plane on mirror image sites. From EPR measurements (3) of Pr pairs in $LaCl_3$ it was concluded that the dominant Pr-Pr interaction was between nearest neighbors along the hexagonal chain and of the form

$$H \simeq J \sum_i (S_x^i S_x^{i+1} + S_y^i S_y^{i+1}).$$

The low temperature ordering properties of

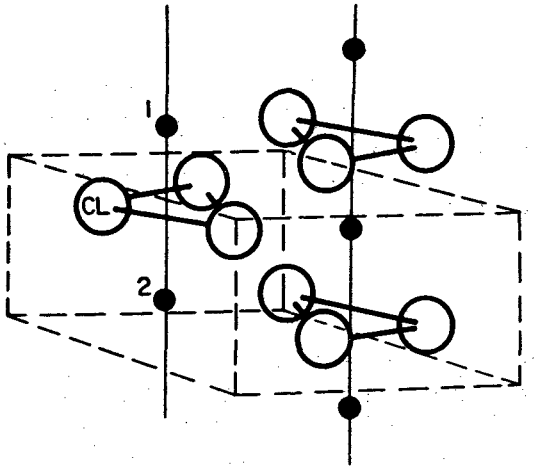

Figure 1. The crystal structure of $PrCl_3$. The solid and open circles represent Pr and Cl ions, respectively. The dashed lines define a unit cell. The vertical lines indicate chains of nearest neighbor Pr ions parallel to the hexagonal axis.

---

*Presented at the 6th Specialized Colloque Ampere on "Quadrupole Interactions and Spatially Resolved NMR in Solids," Crete, Greece, September 12-17, 1983.

$PrCl_3$ are therefore expected to show prominant 1-D XY character. Since the static properties of the XY chain can be calculated, the predicted 1-D character can be tested. This has been done for the specific heat (4) and susceptibility (5). The result for the susceptibility is shown in Figure 2; it shows that the XY model provides an excellent description of the data, at least above 3.6 K. The dynamic properties of the XY chain can also be calculated and the predictions tested using, for example, chlorine magnetic relaxation measurements. Experiments of this type (1) will be reviewed.

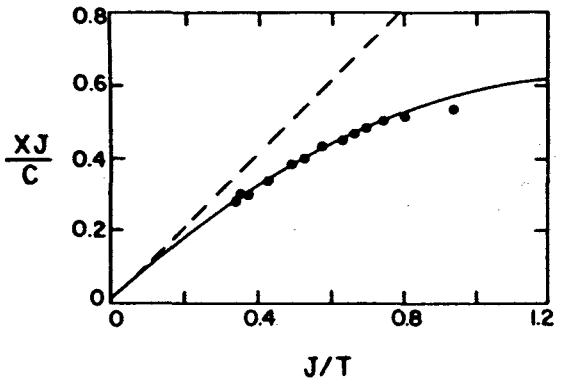

Figure 2. Comparison of experimental susceptibility data with the perpendicular susceptibility of the 1-D XY system (solid curve). The dashed line represents the Curie law for non-interacting dipoles.

Long range ordering occurs in $PrCl_3$ at 0.4 K. Although no direct measurement of the low temperature structure has been performed, the splitting of the chlorine NQR spectrum (5) has been observed in the low temperature phase and this experimental observation has been interpreted (2) to yield a unique and unexpected structure. This work will be discussed.

It is the nature of the Pr ground electronic state in $PrCl_3$ that gives rise to the dominant XY interaction. The ground state electronic configuration of Pr^{3+} is $4f^2\ {}^3H_4$. The Pr^{3+} ion has point symmetry C_{3h} and the resultant crystal field splitting of the low lying manifold gives rise to a non-Kramers ground state doublet separated by 33 cm^{-3} from the first excited state. The ground doublet couples strongly to a Jahn-Teller distortion and this leads to a large XY interaction between Pr sites in an effective spin 1/2 representation (7). This distortion transforms as (x,y) and therefore carries an electric dipole moment; it is represented by the operators S_x,S_y. In addition, the magnetic moment which is small and parallel to the hexagonal axis is responsible for a small $S_z^i S_z^{i+1}$ term.

II. HIGH TEMPERATURE PHASE: DYNAMIC RESPONSE OF A 1-D XY CHAIN (4)

In the high temperature phase all six chlorine sites in the unit cell are equivalent and a single NQR line is observed.

A. Spin-Lattice Relaxation Measurements

Earlier measurements (8) of the spin-lattice relaxation time T_1 were reported for the ^{35}Cl isotope at 4.2 K and below; they are shown in Figure 3. The objective of the more recent measurements (1) was to measure T_1 for both isotopes at a single temperature, 4.2 K, and with sufficient accuracy to identify unambiguously the relaxation mechanism. Figure 4 shows the data for the ^{35}Cl isotope; the straight line is a least squares fit to a single exponential decay function with time constant $T_1 = 4.11 \pm 0.04$ ms. This new value, although more accurate, is consistent with the earlier results. The isotopic ratio of decay constants is $T_1(^{37}Cl)/T_1(^{35}Cl) = 1.38 \pm 0.03$.

In an attempt to explain the spin-lattice relaxation measurements let us assume a magnetic hyperfine mechanism. In a simple model only the Pr ions labeled 1 and 2 in Figure 1 need be considered. Their contribution to T_1^{-1} is

$$T_1^{-1} = (A^2/\hbar)[\Phi_{zz}^{11}(\omega) + \Phi_{zz}^{12}(\omega)]$$

where A is the magnetic hyperfine interaction constant and it is proportional to the chlorine nuclear magnetogyric ratio, γ. The term $A^2/\hbar$ gives the dominant contribution to the isotopic ratio of T_1^{-1} values; with this term only, the predicted ratio is 1.44. The quantities $\Phi_{zz}^{mn}(\omega)$, where ω is the NQR frequency, are given by

$$\Phi_{zz}^{mn}(\omega) = \int_{-\infty}^{\infty} dt\, e^{i\omega t} \langle S_z^m(t) S_z^n(0) \rangle$$

where $\langle S_z m(t) S_z n(0) \rangle$ is the time-dependent, longitudinal correlation function for the electronic spins S^m and S^n. A general expression for this correlation function for the 1-D XY chain exists at all temperatures (9,10).

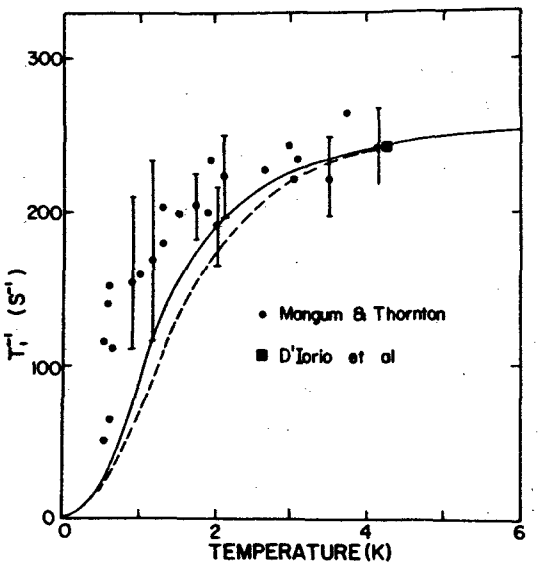

Figure 3. Temperature dependence of the relaxation rate T_1^{-1}. The uncertainty in the D'Iorio et al. data point is given by the size of the symbol. The solid curve represents the theoretical prediction for J= 2.5 K and with the single free parameter chosen to fit the data at 4.2 K; the dashed curve is for J = 2.85 K.

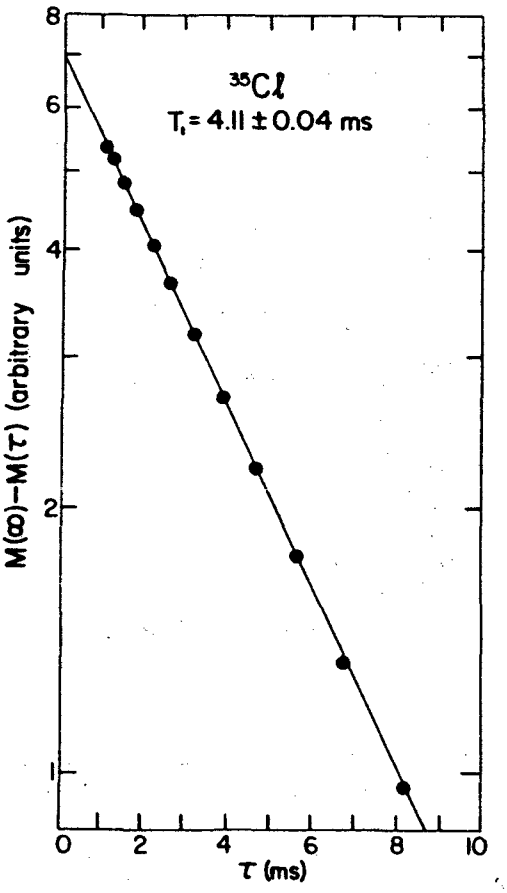

Figure 4. Typical spin-lattice relaxation data at 4.2 K showing exponential decay with time constant T_1.

In the high temperature limit

$$\Phi_{ZZ}{}^{11}(\omega)_{T=\infty} = (\hbar/2\pi J)K(1 - \tilde{\omega}^2/4)$$

where $\tilde{\omega} = \hbar\omega/J$ and K(x) is the complete elliptic integral of the first kind. If only the autocorrelation term is considered

$$\frac{T_1(^{37}Cl)}{T_1(^{35}Cl)} = \left[\frac{\gamma(^{35}Cl)}{\gamma(^{37}Cl)}\right]^2 \frac{K[1 - \tilde{\omega}^2(^{35}Cl)]}{K[1 - \tilde{\omega}^2(^{37}Cl)]}$$

$$= (1.44)(0.98)$$

$$= 1.41$$

In fact, the frequency dependence of the pair correlation function is virtually identical. This result is in good agreement with the measured ratio 1.38 ± 0.03 at 4.2 K.

Using the general expression for the correlation function for a 1-D chain, taking J = 2.5 K and accepting the present 4.2 K value as correct, the theoretical curve shown by the solid line in Figure 3 is deduced. The dashed line is for J = 2.85 which until recently was assumed to be the best available value for this parameter.

The conclusion is that the spin-lattice relaxation is dominated by the magnetic hyperfine interaction and reflects the longitudinal fluctuations of a 1-D XY chain.

B. Spin-Spin Relaxation Measurements

Earlier measurements (8) of the effective spin-spin relaxation time $\hat{T}_2$ were reported for the ^{35}Cl isotope at 4.2 K and below; they are shown in Figure 5. One objective of the more recent measurements (1) was to measure $\hat{T}_2$ for both isotopes at a single temperature, 4.2 K, and with sufficient accuracy to identify unambiguously the relaxation mechanism. Figure 6 shows the data for the ^{35}Cl isotope. Note that the overall decay function is more rapid than exponential. The (dashed) straight line fit to the

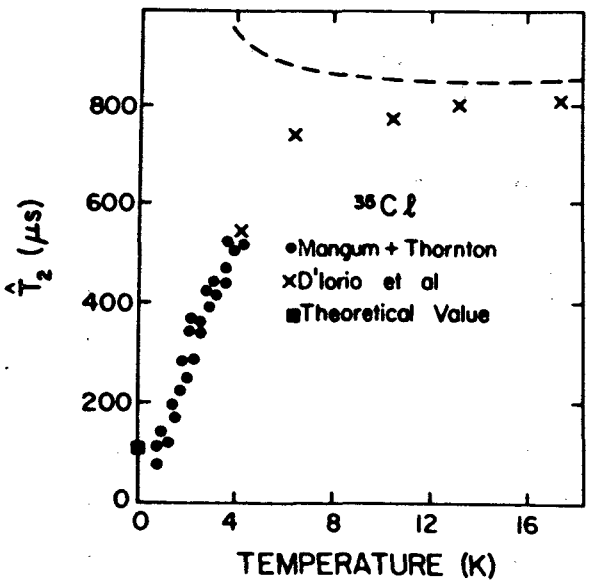

Figure 5. Temperature dependence of the effective spin-spin relaxation time $\hat{T}_2$. The dashed line is the estimated magnetic hyperfine contribution; the data point at T=0 represents the estimated electric hyperfine contribution.

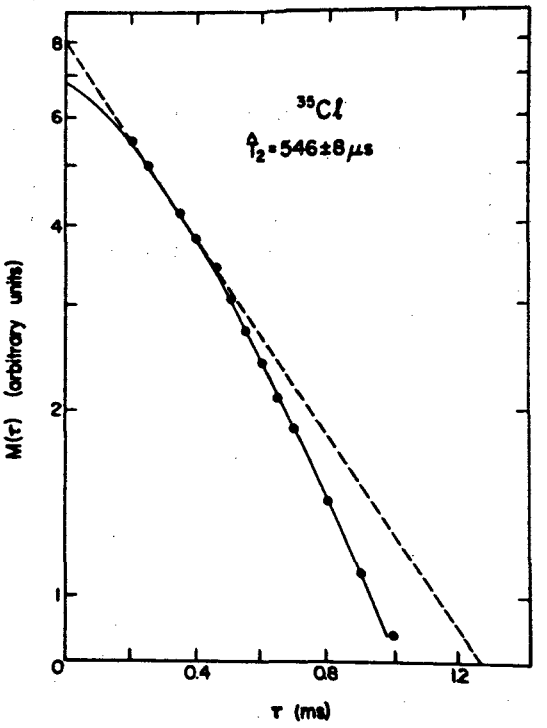

Figure 6. Typical spin-spin relaxation data at 4.2 K showing non-exponential decay. The solid line represents an $\exp(-at^{3/2})$ decay the dashed line an exponential decay with time constant $\hat{T}_2$.

initial part of the dacay represents a single exponential decay function with time constant $\hat{T}_2$ = 546 ± 8 μs. This value, although more accurate, is consistent with the earlier results. The isotopic ratio of decay constants is $\hat{T}_2(^{37}Cl)/\hat{T}_2(^{35}Cl)$ = 1.59 ± 0.04. A second objective of the new measurements was to measure $\hat{T}_2$ at temperatures above 4.2 K. The results are shown in Figure 5; a plateau is reached quite abruptly at about 6 K.

As a first attempt to explain the spin-spin relaxation measurements, let us assume the same magnetic hyperfine mechanism responsible for spin-lattice relaxation. The relaxation rate, T_2^{-1}, is

$$T_2^{-1} = T_1^{-1}/2 + (A^2/\hbar)[\Phi_{zz}^{11}(0) + \Phi_{zz}^{12}(0)]$$

where the $\omega = 0$ terms represent dephasing due to variations in local precession frequencies. This approach fails because the quantity $\Phi_{zz}^{mn}(\omega)$ diverges as ω approaches zero. The conclusion is that the relaxation is non-exponential.

As a second attempt, let us assume the same relaxation mechanism but use a density matrix method (11) to calculate the two pulse echo decay function, $\phi(t)$. Using the value of A determined from the T_1 data, a unique prediction for the temperature dependence of $\hat{T}_2$ can be obtained. This is shown by the dashed line in Figure 5. Although the magnitude of $\hat{T}_2$ at high temperatures is in good agreement with the experimental values, the prediction is for $\hat{T}_2$ to increase at low temperatures whereas, in fact, $\hat{T}_2$ decreases dramatically below 6 K. This second attempt fails at low temperatures.

As a third attempt, an electric quadrupole mechanism is assumed. the transverse Pr moments S_x,S_y physically represent transverse distortions at Pr sites. these moments create electric field gradients at the chlorine sites proportional to S_x,S_y and lead to electric hyperfine interactions of the form $S_x T_m^2$ where T_m^2 is a

second-rank nuclear spin operator. In the simplest model

$$T_1^{-1} \simeq (B^2/\hbar)\Phi_{xx}^{11}(\omega)$$

$$T_2^{-1} \simeq (B^2/\hbar)\Phi_{xx}^{11}(0)$$

where

$$\Phi_{xx}^{11}(\omega) = \int_{-\infty}^{\infty} dt\, e^{i\omega t} \langle S_x^1(t) S_x^1(0) \rangle .$$

At high temperatures (12)

$$\langle S_x^1(t) S_x^1(0) \rangle \sim \exp(-J^2 t^2/4\hbar^2)$$

and

$$T_1^{-1} \simeq T_2^{-1} \simeq \pi^{\frac{1}{2}} B^2/2J\hbar .$$

If B is roughly estimated using a point charge model and the transverse measured transverse electric dipole moment (4), it follows that

$$T_1^{-1} \simeq T_2^{-1} \simeq 1\ s^{-1}$$

which is more than two orders of magnitude slower than the magnetic hyperfine contribution. Electric quadrupole relaxation is ineffective in the high temperature regime both because B is smaller than A and also because the transverse spin correlation function decays more rapidly than the longitudinal correlation function.

At low temperatures, we have seen that the longitudinal correlations become less effective in producing relaxation. In contrast, the transverse correlation function develops a long time tail and in the T = 0 limit (13)

$$\langle S_x^1(t) S_x^1(0) \rangle \sim (\hbar/Jt)^{\frac{1}{2}}$$

Therefore, electric quadrupole relaxation is strongly enhanced at low temperatures. If it dominates at 4.2 K

$$\frac{\hat{T}_2(^{37}Cl)}{\hat{T}_2(^{35}Cl)} \simeq \left[\frac{Q(^{35}Cl)}{Q(^{37}Cl)}\right]^2$$

since the electric hyperfine interaction parameter B is proportional to the nuclear electric quadrupole moment Q. This theoretical ratio has the value 1.61; it is in excellent agreement with the measured ratio 1.59 ± 0.04 at 4.2 K.

Since $\Phi_{xx}^{11}(\omega)$ diverges as ω approaches zero, it is necessary to calculate an echo decay function, $\phi(t)$, and from it deduce $\hat{T}_2$ values. In the low temperature limit

$$\phi(t) \sim \exp[-2B^2(\hbar/J)^{1/2} t^{3/2}].$$

This function is in excellent agreement with the observed decay function at 4.2 K (see solid line in Figure 6).

Lastly, an approximate value of $\hat{T}_2 = 100$ μs is predicted at T = 0; this is the time for an e^{-1} decay of $\phi(t)$ for T = 0. The predicted value is consistent with the values measured at very low temperature as shown in Figure 5.

The conclusion is that at low temperature the spin-spin relaxation is electric quadrupolar in nature and reflects the transverse fluctuations of a 1-D XY chain.

III. LOW TEMPERATURE PHASE: WHAT IS THE ORDERED STRUCTURE?

The ^{35}Cl NQR spectrum as measured in the low temperature phase (6) is illustrated in Figure

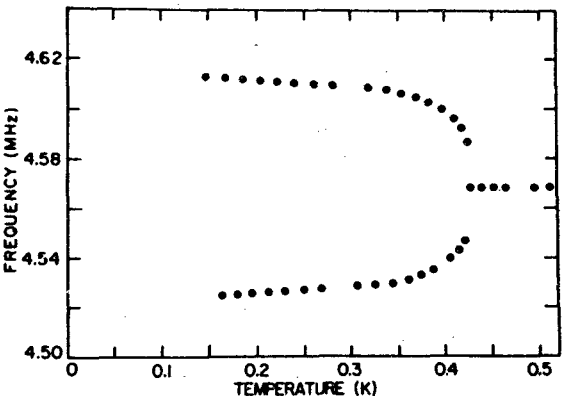

Figure 7. ^{35}Cl NQR spectrum of $PrCl_3$ as measured through the phase transition at 0.4 K.

7. The single line above T_c splits symmetrically into two lines below T_c. The two lines are of equal intensity so that the center of mass of the spectrum is conserved through the transition. Although it was at first assumed that the phase transition resulted from an antiferromagnetic ordering of Pr spins, it was subsequently concluded (14) from an NQR experiment performed in a small Zeeman field that the ordered state was not magnetic. It follows that the transition is structural in origin and presumably due to a cooperative Jahn-Teller distortion (15), but its precise nature is not known.

The observed change in the NQR spectrum places severe constraints on possible space groups of the low temperature structure (2).

Since the phase transition is due to a cooperative Jahn-Teller distortion, the space group of the high temperature phase must be a subgroup of the space group of the high temperature phase. The mathematical theory of symmetry as embodied in the principles of group theory, homotopy theory and representation theory may be used to advantage to discuss this example of a broken symmetry (16-18).

The space group of the high symmetry phase of $PrCl_3$ is C_{6h}^2. The first Brillouin zone is depicted in Figure 8. Its points of symmetry are

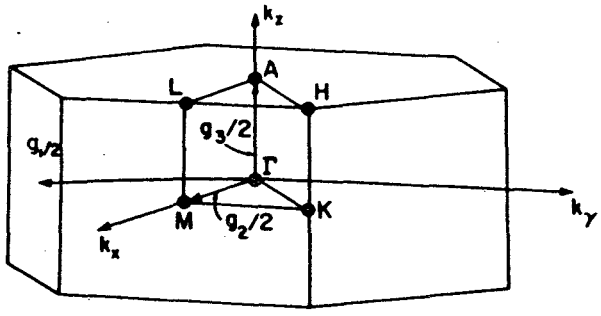

Figure 8. The Brillouin zone of the hexagonal lattice showing the points of symmetry.

Γ, M, A, L, K, and H. Starting from these, the theory of induction allows one to construct all of the commensurate group representations that may be responsible for a commensurate transition. Considering each irreducible representation in turn, representative order parameters and their little groups can be found. Finally, each little group may be identified as a possible space group for the low symmetry phase. Considerations of the site symmetry of the chlorine atoms leads to a classification scheme for the NQR spectra based on such characteristics of the predicted low symmetry phase spectra as the number of lines, their relative intensities, and the conservation or non-conservation of the spectral center of mass.

In fact, there are only two allowed low symmetry structures that are compatible with a two line chlorine NQR spectrum. These are C_{3i}^1 and C_{3h}^1. The C_{3i}^1 structure has a unit cell which is doubled along the hexagonal axis of the C_{6h}^2 structure. The Pr ions no longer have special z coordinates, but since the C_{3i}^1 structure has an inversion center, the Pr ions form equivalent chains with alternating long and short Pr-Pr separations. This structure describes a dimerized state. The C_{3h}^1 structure differs from the C_{6h}^2 structure (Figure 1) through the loss of the inversion center of the unit cell. This would occur if the two Cl triangles experience different expansions/contractions or rotations. The Pr point symmetry remains C_{3h}, but the two Pr ions in each unit cell, and therefore their repsective chains, are nonequivalent.

A choice between the two low temperature structures identified by the group theoretical analysis can be made using physical arguments. The space group C_{3i}^1 is favored for several reasons. We mention only one. A transition to the C_{3h}^1 structure would not remove the electronic degeneracy. The individual chains would retain the symmetry of the high temperature phase, with the difference being that the two nonequivalent chains have slightly different values of the interaction parameter J. In contrast, a transition to the C_{3i}^1 structure *does* remove the electronic degeneracy. An interaction of the form

$$H = J \sum_i (S_x^i S_x^{i+1} + S_y^i S_y^{i+1})$$

implies that at the transition the unit cell will double along the hexagonal axis; the dimerized state is known to be the stable low temperature phase of an XY chain.

The question remains as to why Peierls dimerization occurs in $PrCl_3$ instead of conventional long-range ordering of individual Pr moments. In almost all known quasi 1-D spin systems, interchain interactions are sufficient to establish 3-D long-range order. Although the strength of the interchain interactions is not known in $PrCl_3$, it is not expected to be remarkably small. It is, however, possible that the structure of this compound is such as to hinder the long-range ordering of the transverse moments. The separation between adjacent chains is not large, but interactions between them due to transverse displacements tend to cancel because each Pr ion on one chain is midway between two Pr ions on the adjacent chain. A high degree of cancellation between more distant chains is also expected because of the antiparallel ordering of moments within each chain, the hexagonal lattice structure and the dipolar nature of the long-range interactions.

It is concluded that $PrCl_3$ undergoes a novel type of Peierls dimerization, similar in some respects to the spin-Peierls transition, but different in that the spins involved are not real spins, but pseudospins associated with a Jahn-Teller coupling. Recall that the Peierls transition creates a singlet ground state by opening a gap

between filled and empty states in the electronic excitation spectrum, while in the spin-Peierls transition a similar gap appears in the spin excitation spectrum (19). Nonetheless, the analogy in the spin excitation with the electronic metal-insulator Peierls transition is direct since the dominant Pr-Pr interactions are well described by a 1-D XY coupling which has an exact mathematical transformation to a system of non-interacting fermions. Both the spin dynamics and the phase transition in $PrCl_3$ are almost unique, are of much physical interest, and merit further study at low temperature.

REFERENCES

[1] M. D'Iorio, R. L. Armstrong, and D. R. Taylor, *Phys. Rev.*, **B27,** 1665 (1983).

[2] R. M. Morra, R. L. Armstrong, and D. R. Taylor, *Phys. Rev. Lett.* **51,** 809 (1983).

[3] J. W. Culvahouse, D. P. Schinke, and L. G. Pfortmiller, *Phys. Rev.* **177,** 454 (1969); J. W. Culvahouse and L. G. Pfortmiller, *Bull. Am. Phys. Soc.* **15,** 394 (1970).

[4] J. P. Harrison, J. P. Hessler, and D. R. Taylor, *Phys. Rev.* **B14,** 2979 (1976).

[5] J. T. Folinsbee, J. P. Harrison, D. B. McColl, and D. R. Taylor, *J. Phys.* **C10,** 743 (1977).

[6] J. H. Colwell, B. W. Mangum, and D. B. Utton, *Phys. Rev.* **181,** 842 (1969).

[7] A. Abragam and B. Bleaney, *Electron Paramagnetic Resonance of Transition Ions*, Clarendon Press, Oxford, 1970.

[8] B. W. Mangum and W. D. Thornton, *Phys. Rev. Lett.* **22,** 1105 (1969).

[9] S. Katsura, T. Horiguchi, and M. Suzuki, *Physica* **46,** 67 (1970).

[10] Th. Niemeijer, *Physica* **36,** 377 (1967).

[11] D. R. Taylor and E. Zaremba, *Phys. Rev.* **B23,** 3384 (1981).

[12] J. H. H. Perk and H. W. Capel, *Physica* **89A,** 265 (1977).

[13] H. G. Vaidya and C. A. Tracy, *Physica* **92A,** 1 (1978).

[14] J. P. Hessler and E. H. Carlson, *J. Appl. Phys.* **42,** 1316 (1971).

[15] G. A. Gehring and K. A. Gehring, *Rep. Prog. Phys.* **38,** 1 (1975).

[16] L. Michel, *Rev. Mod. Phys.* **52,** 617 (1980).

[17] M. Sutton and R. L. Armstrong, *Phys. Rev.* **B25,** 1813 (1982); **B27,** 1937 (1983).

[18] M. Sutton and R. L. Armstrong, *J. Magn. Reson.* **47,** 68 (1982).

[19] J. W. Bray, L. V. Interrante, I. S. Jacobs, and J. C. Bonner, in *Extended Linear Chain Compounds*, J. S. Miller, Ed.,Plenum Press, New York, 1982, Vol. 3, pp. 353-415.